

## Optical Control of Peroxisomal Trafficking

Jessica I. Spiltoir,<sup>†</sup> Devin Strickland,<sup>‡</sup> Michael Glotzer,<sup>‡</sup> and Chandra L. Tucker<sup>\*,†</sup>

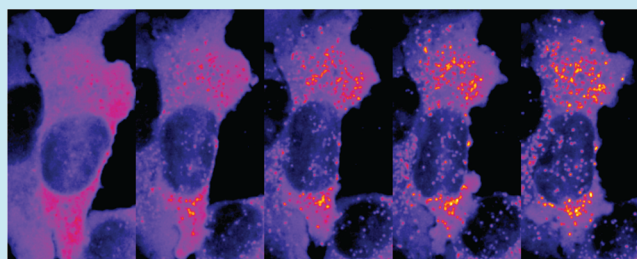
<sup>†</sup>Department of Pharmacology, University of Colorado School of Medicine, Aurora, Colorado 80045, United States

<sup>‡</sup>Department of Molecular Genetics and Cell Biology, University of Chicago, Chicago, Illinois 60637, United States

### S Supporting Information

**ABSTRACT:** The blue-light-responsive LOV2 domain of *Avena sativa* phototropin1 (AsLOV2) has been used to regulate activity and binding of diverse protein targets with light. Here, we used AsLOV2 to photocage a peroxisomal targeting sequence, allowing light regulation of peroxisomal protein import. We generated a protein tag, LOV-PTS1, that can be appended to proteins of interest to direct their import to the peroxisome with light. This method provides a means to inducibly trigger peroxisomal protein trafficking in specific cells at user-defined times.

**KEYWORDS:** optogenetics, LOV domain, caged peptide, peroxisome, trafficking



Peroxisomal targeting is a regulated posttranslational process in which proteins tagged with a peroxisomal targeting signal (PTS1 or PTS2) are selected for import into the peroxisome. The PTS1 targeting signal consists of a short tripeptide (a serine-lysine-leucine “SKL” or similar motif) at the protein C-terminus, which facilitates binding to the Pex5 peroxisomal import receptor. Upon Pex5 binding, cargo are transported from the cytosol to the peroxisomal inner membrane. Studies have shown that attachment of a canonical PTS1 motif to nonperoxisomal proteins, such as GFP, is sufficient for peroxisomal import.<sup>1,2</sup>

In this work, we sought to develop a system to confer light control over peroxisomal protein trafficking. The field of optogenetics involves the use of natural and engineered photosensory domains to confer light control to molecular and cellular processes. Recently, systems have been developed using light to directly regulate protein trafficking, including control of nuclear-cytoplasmic trafficking<sup>3–6</sup> and secretory trafficking.<sup>7</sup> Tools allowing inducible control of peroxisomal import would allow study of the import process or function of specific peroxisomal proteins at specified times and locations. In addition, as proteins imported into the peroxisome are encapsulated in this organelle, such tools could also be applied to functionally sequester proteins from the cytosol at specific times in cells of interest.

To enable optical control of peroxisomal import, we used the LOV2 (Light, Oxygen, Voltage) domain of *Avena sativa* phototropin1 (AsLOV2), a member of the conserved Per-ARNT-Sim (PAS) domain family.<sup>8</sup> In the dark, a C-terminal  $J\alpha$ -helix is bound tightly to the core of AsLOV2.<sup>9</sup> Blue light triggers covalent bond formation between a conserved cysteine residue on the LOV domain and a flavin mononucleotide chromophore.<sup>10,11</sup> This results in unwinding of the  $J\alpha$ -helix and dissociation from the LOV core, ultimately affecting phototropin kinase activity.<sup>9,12,13</sup> These large structural changes

occurring in LOV- $J\alpha$  have been exploited to confer light control over heterologous protein activities.<sup>3,6,14–25</sup> In particular, proteins or peptides attached at the C-terminus of the  $J\alpha$ -helix can be “caged” such that they are unable to interact with effectors in the dark, but this steric block can be released in the presence of light and  $J\alpha$ -helix unwinding.<sup>3,6,14,17,19,21–23,25,26</sup>

Here, we used a similar approach to control binding of a PTS1-tagged protein to the Pex5 peroxisomal import receptor with light (Figure 1a). To first examine feasibility for targeting the LOV-PTS1 fusion to the peroxisome, we used a constitutively active form of AsLOV2 ( $\Delta$ K533) that has a constitutively undocked  $J\alpha$ -helix.<sup>17</sup> We attached a PTS1 sequence from acyl-CoA oxidase, “LQSKL” to the C-terminus of the AsLOV2- $J\alpha$  motif, along with a GFP reporter at the N-terminus to allow visualization. Expression of this construct in COS-7 cells showed a punctate GFP expression pattern consistent with peroxisomal localization (Supporting Information Figure S1). We next tested a  $J\alpha$ -helix truncation series to screen for light dependent peroxisomal targeting (Figure 1b). Within the AsLOV2 domain, we incorporated T406A and T407A mutations that increase  $J\alpha$ -helix docking and a V416I mutation that prolongs the lit state,<sup>17,27,28</sup> as well as G528A and N538E mutations that were shown to increase the dynamic range of a previous LOV-based photoswitch.<sup>16</sup> One of the constructs (PTS1.2) showed no peroxisomal localization in light or dark, while a second (PTS1.3) showed constitutive localization in light and dark. LOV-PTS1.1 (hereafter referred to as LOV-PTS1) showed light-dependent peroxisomal localization, as shown by colocalization of GFP with a peroxisomal marker, PMP70 (Figure 1c).

Received: August 4, 2015

Published: October 29, 2015

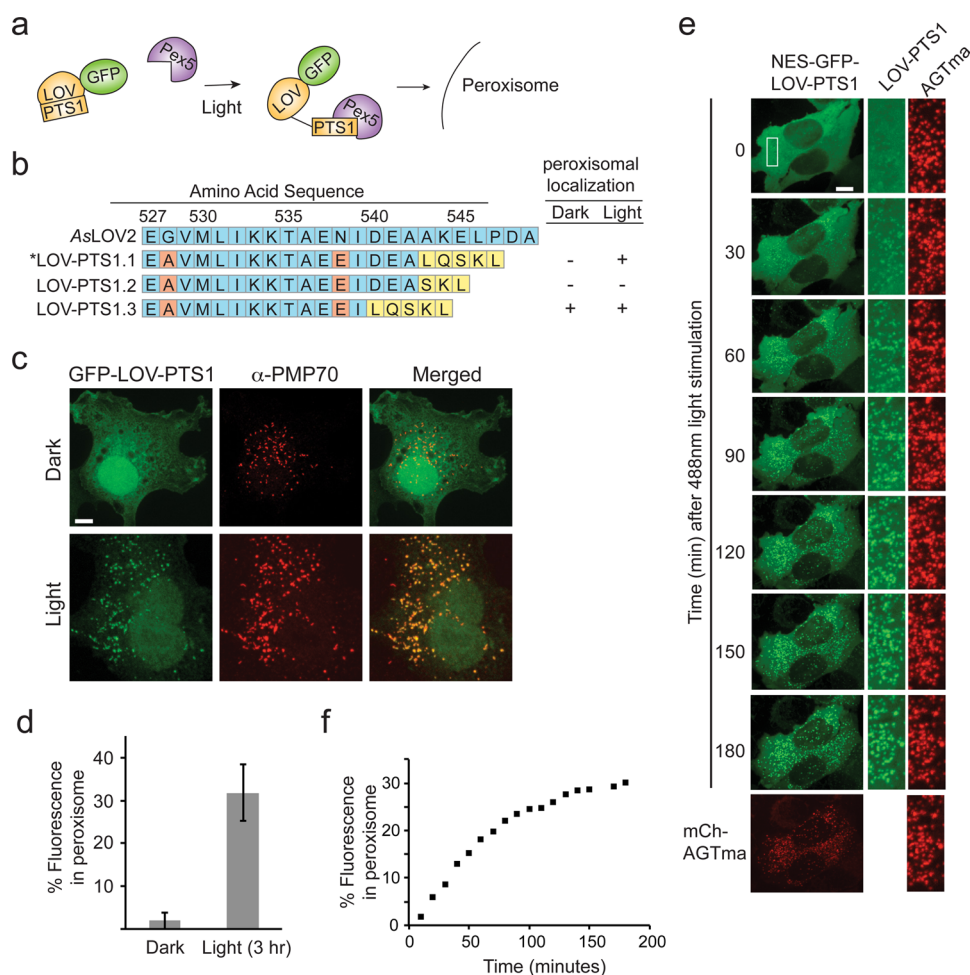


**Figure 1.** Optical regulation of peroxisomal trafficking. (a) Schematic of caged LOV-PTS1 construct. LOV-PTS1 has a C-terminal  $J\alpha$ -helix that dissociates from the LOV core with light and uncages the PTS1 sequence. Pex5 binds PTS1 and shuttles the protein to the peroxisome. (b) Alignment of tested sequences with AsLOV2- $J\alpha$  sequence. Numbering corresponds to amino acid residue in the plant AsLOV2 sequence. LOV-PTS1.1 (\*) was used in further studies. Orange residues indicate regions where mutations were introduced. Yellow residues indicate the PTS1 signal. “+”, < 5% of cells show peroxisomal localization; “-”, greater than 95% of cells show peroxisomal localization. (c) Localization of GFP-LOV-PTS1 in COS-7 cells. COS-7 cells were transfected with GFP-LOV-PTS1 and exposed to dark or blue light pulses for 24 h, 18 h after transfection. Representative fixed cells are shown. Localization of the peroxisomal marker PMP70 is shown in middle. Scale bar, 10  $\mu$ m (d) Quantification of peroxisomal fluorescence in HeLa cells. Cells were transfected with GFP-LOV-PTS1, incubated in dark for 18 h, then imaged every 10 min for 3 h. During imaging, cells were exposed to LED light (1s 461 nm pulse every 1 min). Dark quantification used the image capture at time 0. Data represents the average of one experiment,  $n = 8$ , error bars, s.d. This experiment was repeated two times with similar results. (e) Images of representative HeLa cell expressing NES-GFP-LOV-PTS1 exposed to light using the experimental treatment described in (d). Peroxisomes are highlighted using a mCherry-AGTma reporter. DNA was transfected at a ratio of 3:1 (NES-GFP-LOV-PTS1 to mCherry-AGTma). Scale bar, 10  $\mu$ m. (f) Quantification of image sequence in (e).

Peroxisomal localization of GFP-LOV-PTS1 was minimal in dark, though some background localization could be observed that varied from cell to cell ( $1.9 \pm 1.9\%$  fluorescence in peroxisomes) (Figure 1d). After 3 h light illumination, peroxisomal targeting increased more than 10-fold ( $31.7 \pm 6.5\%$  fluorescence in peroxisomes) (Figure 1d). Using live cell imaging, localization could first be observed  $\sim$ 10–20 min after initial light application (Figure 1e,f and Supporting Information Movie S1), consistent with previous studies in permeabilized or injected cells.<sup>29,30</sup> Peroxisomal localization required sustained delivery of light pulses to maintain AsLOV2 in an activated conformation. Delivery of a single pulse of light, which photostimulates the V416I variant of AsLOV2 with a half-life of  $\sim$ 3 min,<sup>17,27</sup> was insufficient to induce visible peroxisomal targeting (data not shown). The protein may reversibly dissociate from the Pex5 complex upon dark reversion, or the

amount of Pex5 available for binding/translocation may be limited, thus visualization of peroxisomal import is only possible after multiple rounds of Pex5-mediated cargo transport.

To validate that light-dependent import of GFP-LOV-PTS1 was indeed due to light-dependent binding to Pex5, the peroxisomal import receptor, we examined this interaction using yeast two-hybrid (Figure 2). LOV-PTS1 fused to a Gal4 DNA binding domain was tested for interaction with a Pex5-Gal4 activation domain fusion. While LOV-PTS1 and Pex5 did not interact in the dark, they interacted upon blue light illumination (Figure 2b).

We compared import efficacy of the GFP-LOV-PTS1 protein with that of other reporters and AsLOV2 mutants (Figure 3a). In HEK293T cells, GFP-LOV-PTS1 showed  $35.7 \pm 9\%$  of protein localized to peroxisome after 24 h in light, and 10-fold

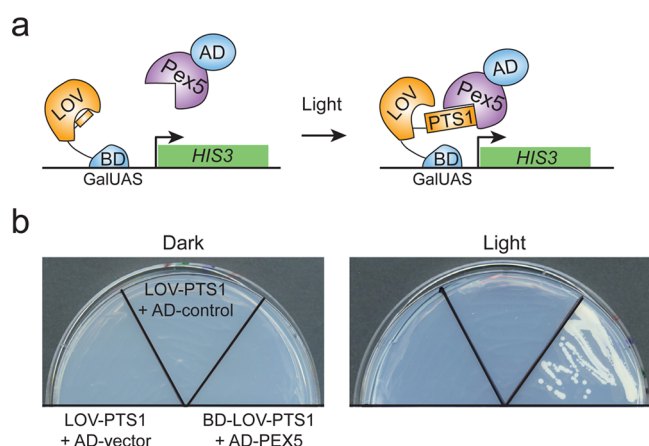


**Figure 2.** Peroxisomal translocation is due to light-dependent binding to Pex5. (a) Schematic showing yeast two-hybrid assay testing interaction of LOV-PTS1 with Pex5. (b) BD-LOV-PTS1 does not interact with AD-Pex5 in the dark, but shows interaction under blue light illumination.

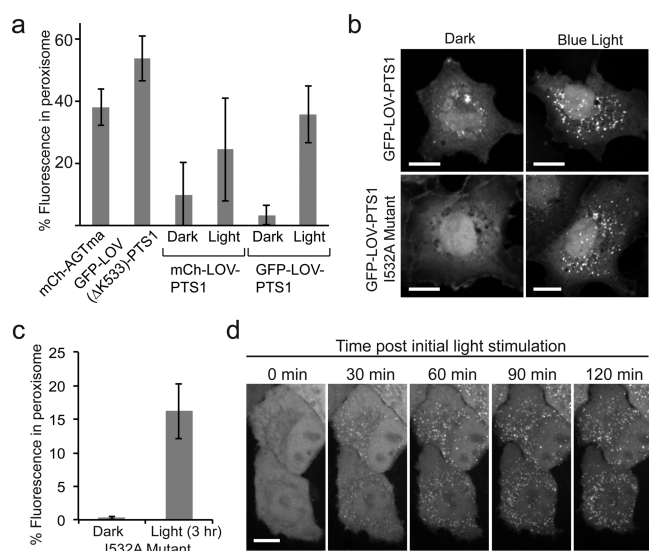


**Figure 3.** Quantification of peroxisomal localization of GFP-LOV-PTS1 mutants and PTS1 reporters. (a) Quantification of % peroxisomal protein. HEK293T cells were transfected with indicated peroxisomal targets and fluorescence quantified after 24 h. Light samples received 24 h blue light pulses. Data represents the average of one imaging experiment,  $n = 8$ , error bars, s.d. (b–d) Analysis of higher caging AsLOV2 mutant I532A. (b) COS-7 cells were transfected with wild-type or I532A GFP-LOV-PTS1 and incubated in dark or 24 h light. Scale bar, 10  $\mu\text{m}$  (c) Quantification of peroxisomal localization in HeLa cells transfected with GFP-LOV-PTS1(I532A). Cells were incubated in dark 18 h, then treated with light pulses and imaged for GFP fluorescence every 5 min for 3 h. The first image was used to quantify dark background. Data represents the average of one imaging experiment,  $n = 7$ , error bars, s.d. This experiment was repeated two times with similar results. (d) Image series of cells expressing GFP-LOV-PTS1(I532A) treated as in (c).

lower levels in dark ( $3.3 \pm 3\%$ ). With the GFP-LOV-PTS1 $\Delta$ K533 variant,  $53 \pm 7\%$  of the protein was localized in the peroxisome after 24 h. A mCherry-tagged native peroxisomal protein, alanine: glyoxylate aminotransferase (mCherry-AGTma), showed lower efficacy of import ( $38 \pm 6\%$  peroxisomal). A mCherry-tagged version of LOV-PTS1 (mCh-LOV-PTS1) showed light/dark differences, but much

higher background in dark and reduced import in light, thus further experiments used only the GFP-tagged version. As the GFP-LOV-PTS1 construct showed some background peroxisomal import even in the dark, we tested whether we could reduce this using a I532A AsLOV2 variant previously shown to stabilize dark state  $\text{J}\alpha$ -helix docking.<sup>16</sup> Incorporation of this mutant eliminated background peroxisomal localization in the dark, but also reduced light-stimulated translocation ( $16.2 \pm 4\%$  fluorescence in the peroxisome after 3 h light), consistent with the higher overall caging properties of this mutant (Figure 3b–d). Given the successful use of I532A in reducing dark state binding here, as well as in several prior studies with AsLOV2,<sup>16,17</sup> this residue may be universally useful for toggling the dynamic range of a variety of LOV-based photoswitches.

As the I532A mutant showed very low background, we examined if we could use our light-regulated system to follow the fate of peroxisomal cargo (Supporting Information Figure S2). We induced peroxisomal accumulation of GFP-LOV-(I532A)-PTS1 by incubating with light for 18 h, then blocked accumulation with a 24 h dark chase. Samples incubated in dark the entire 48 h showed minimal (0.5%) peroxisomal accumulation, indicating this approach should provide a useful means to track protein specifically targeted to the peroxisome only when light is applied. We observed no significant difference in levels of peroxisomal protein between cells quantified at the start of the dark incubation or after 24 h in dark, indicating that fractions in the cytosol and peroxisome remained relatively stable over this period.

One potential application of a light-regulated trafficking signal is to sequester a protein of interest from the cytosol, an approach that has been used with other optogenetic tools.<sup>3–6,31</sup> To examine this, we tested depletion of cytosolic protein from cells expressing GFP-LOV-PTS1 from a tetracycline responsive promoter (Figure 4). When coexpressed with a tTA (Tet-OFF)

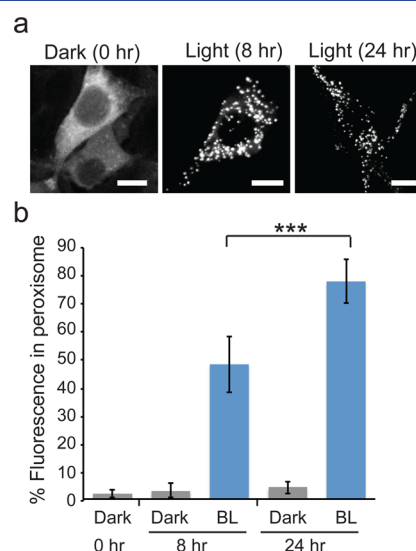


**Figure 4.** Light-triggered depletion of a cytosolic reporter protein. HEK293T cells expressing pTRE3G-NES-GFP-LOV-PTS1 and pBT224-tTA2 were incubated in the dark for 18 h, then doxycycline (1  $\mu\text{g}/\text{mL}$ ) was added and light treatment was initiated. (a) Images of representative cells 0, 8, and 24 h after initiation of light treatment. Scale bar, 10  $\mu\text{m}$ . (b) Quantification of percent peroxisomal protein at 0, 8, or 24 h. Data represents average of one experiment; this experiment was repeated 2 times with similar results.  $n = 10$ , error bars, s.d. \*\*\*,  $p$ -value  $< 0.001$ .

transcriptional activator, this allows blockage of transcription with doxycycline. This construct also contained a nuclear export sequence to maintain cytosolic localization. We induced expression of GFP-LOV-PTS1 in dark, then added doxycycline to block transcription and light to induce peroxisomal trafficking. While minimal peroxisomal localization ( $1.9 \pm 1.3\%$  at time 0) was observed in dark, samples incubated in light showed depletion of cytosolic protein into the peroxisome ( $77 \pm 7.6\%$  of protein localized to the peroxisome after 24 h). Depletion was dose-dependent, increasing with duration of light incubation.

Prior studies have indicated that proteins imported into the peroxisome can allow import of “piggybacking” binding proteins.<sup>32–34</sup> We thus tested if this approach could be extended to deplete interacting proteins from the cytosol. We tagged GFP-LOV-PTS1 with FKBP12, which was coexpressed with a mCherry-labeled FRB (mCh-FRB) (Figure 5a). FRB

peroxisomal trafficking of FKBP-GFP-LOV-PTS1 could be triggered by light (Figure 5b). In contrast, when coexpressed with FRB-mCh and rapamycin was added prior to light, peroxisomal translocation was prevented. Rapamycin itself had no effect on peroxisomal trafficking in the absence of mCh-FRB (Figure 5b). These observations demonstrate that binding of a second protein to a PTS1-tagged cargo, per se, is not sufficient to allow trafficking of any protein. Thus, other criteria are important for import of oligomeric proteins or protein complexes. This data correlates with recent work suggesting peroxisomal import of many oligomeric proteins is often inefficient.<sup>36</sup> Although we cannot exclude the possibility that binding to FRB-mCh sterically blocks the interaction of LOV-PTS1 with Pex5, our results suggest that, in some cases, a binding interaction may prevent or block peroxisomal import of a PTS1-tagged cargo.

In summary, we demonstrate use of the AsLOV2 domain to directly control peroxisomal import with light. The construct showing the best light/dark differences used a fusion site on the J $\alpha$ -helix (after Ala542) similar to that used with TULIP dimerizers.<sup>17</sup> Other studies have successfully caged peptides using nearby fusion sites, such as nuclear localization peptides caged using fusions at Ile539, Asp540, or (to cage a bipartite NLS), Lys544.<sup>3,6</sup> A fusion site at Ala543 was successful for caging a ssrA peptide<sup>21</sup> and a “RRRG” degron sequence,<sup>14</sup> while a kinase inhibitor was caged at a junction with Glu541.<sup>26</sup> Combined, these results indicate a clear consensus for successful caging of peptide fusions between residues 539–544 of the J $\alpha$ -helix; however, optimal placement appears to differ within these sites depending on the peptide used.

We were unable to completely deplete cytosolic protein using this approach after 24 h, suggesting some inefficiency and saturation of the import process. We were also unable to sequester interacting proteins into the peroxisome, suggesting that there are specific requirements to “piggybacking” proteins into this organelle. Indeed, using a dual chemical and light regulated approach, we found that binding to a second cytosolic protein prevented peroxisomal import of a competent PTS1-tagged cargo. Binding to cytosolic proteins may provide a means for regulation of compartmentalization for dual localized proteins (for example, proteins that localize either to the peroxisome or mitochondria under different conditions). Similar mechanisms of binding interactions preventing import could also contribute to disease states associated with mislocalization of peroxisomal proteins, as in the metabolic disease primary hyperoxaluria.<sup>37</sup>

We envision this tool may be used to inducibly target proteins to the peroxisome at specific times or within defined locations, to study kinetics of peroxisomal import, and to track peroxisomal cargo. This approach can also be used to deplete protein from the cytosol; however, this process is slow, occurring over a time frame of hours, and over the time frame of our study did not allow complete protein knockdown. Relatively slow time scales such as these, however, are comparable to other approaches to deplete protein activity with light such as inducible degradation.<sup>14,19</sup> While we did not specifically explore this application, given the saturability of the peroxisomal import machinery,<sup>30</sup> we expect the GFP-LOV-PTS1 module may also have utility in competition experiments, allowing blockage of protein import at specific times and locations.

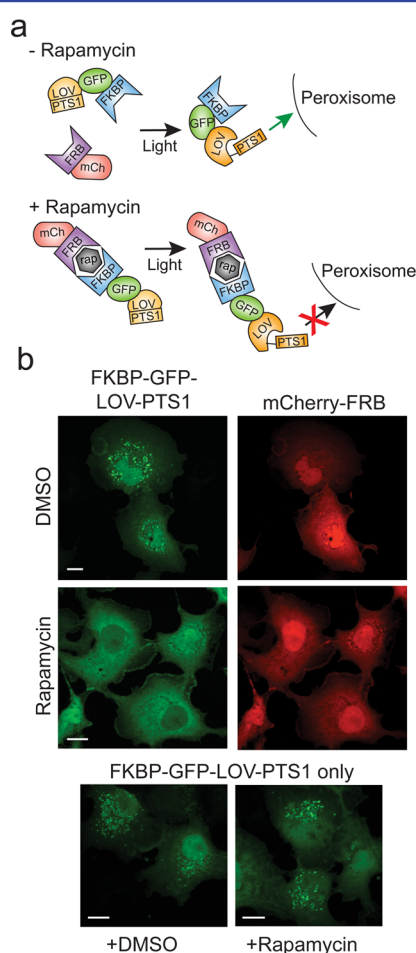


**Figure 5.** Rapamycin-induced dimerization blocks light-triggered peroxisomal import of GFP-LOV-PTS1. (a) Schematic of constructs used. (b) When coexpressed in COS-7 cells with mCherry-FRB, FKBP-tagged GFP-LOV-PTS1 is inducibly targeted to the peroxisome with light, but targeting is blocked if rapamycin, which induces FRB-FKBP dimerization, is added first. Constructs were transfected at a ratio of 2:1 (FKBP-GFP-LOV-PTS1 to mCherry-FRB). Translocation of FKBP-GFP-LOV-PTS1 expressed alone is not affected by rapamycin. Scale bar, 10  $\mu$ m.

and FKBP do not interact when coexpressed but dimerize in the presence of rapamycin.<sup>35</sup> When expressed alone or coexpressed with mCh-FRB in the absence of rapamycin,

## METHODS

### 1. Chemicals, Strains, and Plasmid Construction.

Primer and final clone sequences are listed in [Supporting Information Table S1](#). Rapamycin was from Selleck Chemical LLC, doxycycline hyclate was from Enzo. We used PCR to amplify the “TULIP” LOVpep construct pDS248,<sup>17</sup> containing an erbin binding peptide at the C-terminus of GFP-AsLOV2- $\alpha$ . This construct contains residues 404–540 of AsLOV2 (numbering corresponds to the corresponding location in the wild-type *Arabidopsis* phototropin 1 sequence), as well as additional mutations T406A, T407A, and V416 in the AsLOV2 core. In addition, we added helix-stabilizing mutations G528A and N538E. A canonical PTS1 peroxisomal targeting sequence, “LQSKL”, was added at the C-terminus. To generate the constitutively active  $\Delta$ K533 variant, we used pDS420 as template.<sup>17</sup> The GFP-LOV-PTS1 insert was cloned into pcDNA3.1 at *Bam*HI and *Eco*RI sites, using primers 1068f/1070r (LOV-PTS1.1), 1068f/1072 (LOV-PTS1.2), 1068f/1071r (LOV-PTS1.3), or 1068f/1069r (LOV-PTS1-CA). To create a tetracycline regulated construct, a nuclear export signal was cloned into pcDNA3.1-GFP-LOV-PTS1 at *Hind*III and *Bam*HI to create pcDNA3.1-NES-GFP-LOV-PTS1. NES-GFP-LOV-PTS1 was PCR-amplified and cloned into pTRE3G-luc between *Sal*I and *Eco*NI using primers 1713f/1714r. Site directed mutagenesis was used to change Ile532 to Ala using primers 1567f/1568r. The mCherry-AGTma construct was generated by first inserting mCherry into pcDNA3.1 between *Bam*HI and *Eco*RI using primers 1347f/1373r, and then inserting the coding sequence for alanine: glyoxylate aminotransferase at *Eco*RV and *Xho*I using 1548f/1541r. For yeast two-hybrid studies, the Gal4AD-Pex5 fusion protein was in pGADT7rec (Clontech). LOV-PTS1 was cloned by homologous recombination in pDBTrp<sup>38</sup> using primers 1084f/1085r. The mCherry-FRB construct was generously provided by Dr. Matthew Kennedy (UC Denver). 2xFKBP was amplified from 2xFKBP-GFP-homer1c (provided by Dr. Kennedy) by PCR and cloned into the pcDNA3.1-GFP-LOV-PTS1.1 vector at *Kpn*I and *Bam*HI sites.

**2. Indirect Immunofluorescence.** HEK293T and COS-7 cells were fixed with 4% paraformaldehyde, permeabilized with 0.2% Triton X-100 in PBS with 5% normal goat serum, and incubated with an  $\alpha$ -PMP70 monoclonal antibody (Sigma clone 70–18, SAB4200181, 1:100 dilution) and Cy3-conjugated goat antimouse secondary antibody (Jackson ImmunoResearch 115–165–146, 1:500 dilution).

**3. Microscopy, Live Cell Imaging, and Image Analysis.** Media in glass bottom dishes was changed to HBS with 1 mM  $\text{CaCl}_2$  directly before imaging. Live cell imaging was performed at 34 °C using two systems: 1) An Olympus IX71 microscope equipped with a spinning disc scan head (Yokogawa Corporation) with a 60 $\times$ /NA 1.4 objective. Excitation illumination was delivered from an AOTF controlled laser launch (Andor Technology) and images collected on a 1024  $\times$  1024 pixel EM-CCD camera (iXon; Andor Technology). The emission bandpass filters were 525/30 (GFP), and 685/36 (mCherry). Metamorph software was used for collection of images. To focus on cells without stimulating, we used filtered light (572/28 bandpass filter, Chroma).

2) A Zeiss AxioObserver Z1 Inverted Spinning Disc microscope with a 63 $\times$ /NA 1.4 objective and HQ 480/40 $\times$  and HQ565/30 $\times$  (Chroma) bandpass filters. Excitation illumination was delivered by a 3i Ablate! Model 3iL13 and

image collected using a Yokogawa CSU-X1CU camera. Slidebook 6 was used for image collection.

ImageJ 1.45s and Fiji were used for image analysis. Percent of protein in puncta was calculated by first determining the total fluorescence within the cell or cell region and subtracting background. Then, the total fluorescence within peroxisomal puncta (background subtracted as well as determined using ImageJ thresholding (Otsu’s method) to delineate protein within puncta (also background subtracted). The % fluorescence within peroxisomes was calculated by dividing the fluorescence within puncta by total fluorescence within each cell or analyzed region.

**4. Cell Culture Studies.** HeLa, HEK293T, and COS-7 cells were maintained in Dulbecco’s modified Eagle medium (DMEM) supplemented with 10% FBS and 1% penicillin-streptomycin at 37 °C with 5%  $\text{CO}_2$ . Cells were seeded onto a 35 mm glass bottom dish (live cell imaging) or coverslips on a 12 well plate (fixed images) and transfected using Lipofectamine 2000 (Invitrogen) according to the manufacturer’s protocol. For Tet-OFF experiments ([Figure 4](#)), cells were transfected with pTRE3G-NES-GFP-LOV-PTS1 and pBT224-tTA2 at a DNA ratio of 1:1. Eighteen hours after transfection, 1  $\mu\text{g}/\text{mL}$  doxycycline was added to the media. Dark samples were wrapped in aluminum foil immediately after transfection, and all manipulations carried out using a red safelight. Unless otherwise indicated, light-treated cells were illuminated using a custom programmable blue LED light source (461 nm) with a 1 s pulse per 1 min interval, 5.8  $\text{mW}/\text{cm}^2$ .

**5. Yeast Studies.** Yeast two-hybrid studies were performed using strain AH109 (MATa, *trp1*–901, *leu2*–3, 112, *ura3*–52, *his3*–200, *gal4* $\Delta$ , *gal80* $\Delta$ , *LYS2::GAL1<sub>UAS</sub>-GAL1<sub>TATA</sub>-HIS3*, *GAL2<sub>UAS</sub>-GAL2<sub>TATA</sub>-ADE2*, *URA3::MEL1<sub>UAS</sub>-MEL1<sub>TATA</sub>-lacZ*, *MEL1*). Yeast were transformed with indicated GalBD and GalAD fusion plasmids, then grown on SC -Trp/-Leu/-His/ + 3 mM 3-AT for 3 days at 30 °C in light or dark. The AD-control was a pGADT7rec-CIB1 construct that is not expected to bind Pex5.

## ASSOCIATED CONTENT

### Supporting Information

The Supporting Information is available free of charge on the ACS Publications website at DOI: 10.1021/acssynbio.5b00144.

Movie S1. Light-triggered peroxisomal translocation of GFP-LOV-PTS1. HeLa cells expressing GFP-LOV-PTS1 were exposed to blue light at the start of the movie ( $t = 0$ ). Images were acquired every 10 min for 3 h. ([AVI](#))  
Table S1. Sequences of constructs and primers used in cloning. ([XLS](#))

Figure S1. Constitutive trafficking to peroxisomes using a LOV2 variant. A GFP-LOV-PTS1-CA fusion protein carrying a mutation that eliminates  $\text{J}\alpha$ -helix docking ( $\Delta$ K533) shows peroxisomal localization even without blue light. Scale bar, 5  $\mu\text{m}$ . ([PDF](#))

Figure S2. Tracking peroxisomal trafficked cargo. Quantification of peroxisomal localization in HEK293 cells transfected with GFP-LOV-PTS1(I532A). Cells were either incubated in dark for the 48 h (“Dark”), or in dark for 6 h, then in light for 18 h to induce peroxisomal import. Samples were quantified at this time (0 h), or after an additional 24 h dark incubation (24 h). Data represents the average of one experiment,  $n = 8$ , error

bars, s.d. N.S.,  $p > 0.05$ . This experiment was repeated two times with similar results. (PDF)

## AUTHOR INFORMATION

### Corresponding Author

\*E-mail: [chandra.tucker@ucdenver.edu](mailto:chandra.tucker@ucdenver.edu).

### Author Contributions

J.I.S. carried out experimental studies, analyzed data, and wrote the manuscript. C.L.T. conceived and directed the studies, analyzed data, and wrote and edited the manuscript. D.S. and M.G. shared unpublished data and reagents and provided guidance on studies.

### Notes

The authors declare no competing financial interest.

## ACKNOWLEDGMENTS

We thank Dr. Matthew Kennedy (UC Denver) for providing mCherry-FRB and 2xFKBP, and for helpful suggestions on the manuscript, and Liqun Luo for providing pBT224-tTA2 (obtained through Addgene). This work was funded by grants from the National Institutes of Health (GM100225, DK081584) to C.L.T., and by funds from the University of Colorado.

## REFERENCES

- (1) Gould, S. G., Keller, G. A., and Subramani, S. (1987) Identification of a peroxisomal targeting signal at the carboxy terminus of firefly luciferase. *J. Cell Biol.* 105, 2923–31.
- (2) Gould, S. J., Keller, G. A., Hosken, N., Wilkinson, J., and Subramani, S. (1989) A conserved tripeptide sorts proteins to peroxisomes. *J. Cell Biol.* 108, 1657–64.
- (3) Niopek, D., Benzinger, D., Roensch, J., Draebing, T., Wehler, P., Eils, R., and Di Ventura, B. (2014) Engineering light-inducible nuclear localization signals for precise spatiotemporal control of protein dynamics in living cells. *Nat. Commun.* 5, 4404.
- (4) Crefcoeur, R. P., Yin, R., Ulm, R., and Halazonetis, T. D. (2013) Ultraviolet-B-mediated induction of protein-protein interactions in mammalian cells. *Nat. Commun.* 4, 1779.
- (5) Yang, X., Jost, A. P.-T., Weiner, O. D., and Tang, C. (2013) A light-inducible organelle-targeting system for dynamically activating and inactivating signaling in budding yeast. *Mol. Biol. Cell* 24, 2419–30.
- (6) Yumerefendi, H., Dickinson, D. J., Wang, H., Zimmerman, S. P., Bear, J. E., Goldstein, B., Hahn, K., and Kuhlman, B. (2015) Control of Protein Activity and Cell Fate Specification via Light-Mediated Nuclear Translocation. *PLoS One* 10, e0128443.
- (7) Chen, D., Gibson, E. S., and Kennedy, M. J. (2013) A light-triggered protein secretion system. *J. Cell Biol.* 201, 631–40.
- (8) Möglich, A., Ayers, R. A., and Moffat, K. (2009) Structure and signaling mechanism of Per-ARNT-Sim domains. *Structure* 17, 1282–94.
- (9) Harper, S. M., Neil, L. C., and Gardner, K. H. (2003) Structural basis of a phototropin light switch. *Science (Washington, DC, U. S.)* 301, 1541–1544.
- (10) Swartz, T. E., Corchnoy, S. B., Christie, J. M., Lewis, J. W., Szundi, I., Briggs, W. R., and Bogomolni, R. A. (2001) The photocycle of a flavin-binding domain of the blue light photoreceptor phototropin. *J. Biol. Chem.* 276, 36493–500.
- (11) Salomon, M., Christie, J. M., Knieb, E., Lempert, U., and Briggs, W. R. (2000) Photochemical and mutational analysis of the FMN-binding domains of the plant blue light receptor, phototropin. *Biochemistry* 39, 9401–9410.
- (12) Halavaty, A. S., and Moffat, K. (2007) N- and C-terminal flanking regions modulate light-induced signal transduction in the

LOV2 domain of the blue light sensor phototropin 1 from *Avena sativa*. *Biochemistry* 46, 14001–14009.

- (13) Harper, S. M., Christie, J. M., and Gardner, K. H. (2004) Disruption of the LOV- $\alpha$  helix interaction activates phototropin kinase activity. *Biochemistry* 43, 16184–92.

- (14) Bonger, K. M., Rakhit, R., Payumo, A. Y., Chen, J. K., and Wandless, T. J. (2014) General method for regulating protein stability with light. *ACS Chem. Biol.* 9, 111–5.

- (15) Strickland, D., Moffat, K., and Sosnick, T. R. (2008) Light-activated DNA binding in a designed allosteric protein. *Proc. Natl. Acad. Sci. U. S. A.* 105, 10709–10714.

- (16) Strickland, D., Yao, X., Gawlak, G., Rosen, M. K., Gardner, K. H., and Sosnick, T. R. (2010) Rationally improving LOV domain-based photoswitches. *Nat. Methods* 7, 623–626.

- (17) Strickland, D., Lin, Y., Wagner, E., Hope, C. M., Zayner, J., Antoniou, C., Sosnick, T. R., Weiss, E. L., and Glotzer, M. (2012) TULIPS: tunable, light-controlled interacting protein tags for cell biology. *Nat. Methods* 9, 379–384.

- (18) Schmidt, D., Tillberg, P. W., Chen, F., and Boyden, E. S. (2014) A fully genetically encoded protein architecture for optical control of peptide ligand concentration. *Nat. Commun.* 5, 3019.

- (19) Renicke, C., Schuster, D., Usherenko, S., Essen, L.-O., and Taxis, C. (2013) A LOV2 domain-based optogenetic tool to control protein degradation and cellular function. *Chem. Biol.* 20, 619–26.

- (20) Lee, J., Natarajan, M., Nashine, V. C., Socolich, M., Vo, T., Russ, W. P., Benkovic, S. J., and Ranganathan, R. (2008) Surface sites for engineering allosteric control in proteins. *Science (Washington, DC, U. S.)* 322, 438–442.

- (21) Lungu, O. I., Hallett, R. A., Choi, E. J., Aiken, M. J., Hahn, K. M., and Kuhlman, B. (2012) Designing photoswitchable peptides using the AsLOV2 domain. *Chem. Biol.* 19, 507–517.

- (22) Wu, Y. I., Frey, D., Lungu, O. I., Jaehrig, A., Schlichting, I., Kuhlman, B., and Hahn, K. M. (2009) A genetically encoded photoactivatable Rac controls the motility of living cells. *Nature* 461, 104–108.

- (23) Pham, E., Mills, E., and Truong, K. (2011) A synthetic photoactivated protein to generate local or global Ca(2+) signals. *Chem. Biol.* 18, 880–90.

- (24) Rao, M. V., Chu, P.-H., Hahn, K. M., and Zaidel-Bar, R. (2013) An optogenetic tool for the activation of endogenous diaphanous-related formins induces thickening of stress fibers without an increase in contractility. *Cytoskeleton* 70, 394–407.

- (25) Guntas, G., Hallett, R. A., Zimmerman, S. P., Williams, T., Yumerefendi, H., Bear, J. E., and Kuhlman, B. (2015) Engineering an improved light-induced dimer (iLID) for controlling the localization and activity of signaling proteins. *Proc. Natl. Acad. Sci. U. S. A.* 112, 112–7.

- (26) Yi, J. J., Wang, H., Vilela, M., Danuser, G., and Hahn, K. M. (2014) Manipulation of Endogenous Kinase Activity in Living Cells using Photoswitchable Inhibitory Peptides. *ACS Synth. Biol.* 3, 788.

- (27) Zoltowski, B. D., Vaccaro, B., and Crane, B. R. (2009) Mechanism-based tuning of a LOV domain photoreceptor. *Nat. Chem. Biol.* 5, 827–834.

- (28) Zayner, J. P., Antoniou, C., and Sosnick, T. R. (2012) The amino-terminal helix modulates light-activated conformational changes in AsLOV2. *J. Mol. Biol.* 419, 61–74.

- (29) Walton, P. A., Gould, S. J., Feramisco, J. R., and Subramani, S. (1992) Transport of microinjected proteins into peroxisomes of mammalian cells: inability of Zellweger cell lines to import proteins with the SKL tripeptide peroxisomal targeting signal. *Mol. Cell. Biol.* 12, 531–41.

- (30) Wendland, M., and Subramani, S. (1993) Cytosol-dependent peroxisomal protein import in a permeabilized cell system. *J. Cell Biol.* 120, 675–85.

- (31) Lee, S., Park, H., Kyung, T., Kim, N. Y., Kim, S., Kim, J., and Do Heo, W. (2014) Reversible protein inactivation by optogenetic trapping in cells. *Nat. Methods* 11, 633.

- (32) Islinger, M., Li, K. W., Seitz, J., Völkl, A., and Lüers, G. H. (2009) Hitchhiking of Cu/Zn superoxide dismutase to peroxisomes–

evidence for a natural piggyback import mechanism in mammals. *Traffic* 10, 1711–21.

(33) McNew, J. A., and Goodman, J. M. (1994) An oligomeric protein is imported into peroxisomes in vivo. *J. Cell Biol.* 127, 1245–57.

(34) Glover, J. R., Andrews, D. W., and Rachubinski, R. A. (1994) Saccharomyces cerevisiae peroxisomal thiolase is imported as a dimer. *Proc. Natl. Acad. Sci. U. S. A.* 91, 10541–5.

(35) Spencer, D. M., Wandless, T. J., Schreiber, S. L., and Crabtree, G. R. (1993) Controlling signal transduction with synthetic ligands. *Science (Washington, DC, U. S.)* 262, 1019–1024.

(36) Freitas, M. O., Francisco, T., Rodrigues, T. A., Lismont, C., Domingues, P., Pinto, M. P., Grou, C. P., Fransen, M., and Azevedo, J. E. (2015) The peroxisomal protein import machinery displays a preference for monomeric substrates. *Open Biol.* 5, 140236.

(37) Danpure, C. J., Cooper, P. J., Wise, P. J., and Jennings, P. R. (1989) An enzyme trafficking defect in two patients with primary hyperoxaluria type 1: peroxisomal alanine/glyoxylate aminotransferase rerouted to mitochondria. *J. Cell Biol.* 108, 1345–1352.

(38) Tucker, C. L., Peteya, L. A., Pittman, A. M., and Zhong, J. (2009) A genetic test for yeast two-hybrid bait competency using RanBPM. *Genetics* 182, 1377–1379.